Ramesh Kaul[1]
S. Banumathi[2]
D. Velmurugan[2]
R. Balaji Rao[3]
P. Balaram[1]

[1] Molecular Biophysics Unit,
Indian Institute of Science,
Bangalore-560 012, India

[2] Department of
Crystallography and
Biophysics,
University of Madras,
Chennai-600 025, India

[3] Department of Chemistry,
Banaras Hindu University,
Varanasi-221 005, India

Conformational Choice at α,α-Di-*n*-Propylglycine Residues: Helical or Fully Extended Structures?

Abstract: *The conformational analysis of peptides containing a single α,α-di-n-propylglycine (Dpg) residue incorporated into valine-rich sequences has been undertaken in order to delineate the possible role of sequence effects in stabilizing fully extended (C_5) or local helical conformations at this residue. The three peptides Boc–Val–Dpg–Val–OMe (3), Boc–Val–Val–Dpg–Val–OMe (4), Boc–Val–Val–Dpg–Val–Val–OMe (5), have been studied by ^{1}H-nmr methods in chloroform (CDCl$_3$) and dimethylsulfoxide (DMSO) solutions. Even in a relatively poorly solvating medium like CDCl$_3$, all the valine NH groups appear to be solvent-exposed, suggesting an absence of folded β-turn conformations. However, in both CDCl$_3$ and DMSO the Dpg NH groups in all the three peptides appear to behave like apparently solvent-inaccessible groups. In fully extended C_5 conformations, the proximity of the NH and CO groups of Dpg may preclude effective solvation due to a combination of stereoelectronic factors. Nuclear Overhauser effects provide support for the largely extended backbones. The crystal structure of peptide 3 reveals an extended conformation at Dpg (2) with φ = −176°, ψ = 180°. A correlation between the crystallographically observed backbone conformation and solution nmr parameters in DMSO has been attempted using available data. Dpg residues placed in poor helix stabilizing environments may be expected to favor a local C_5 conformation.* © 2000 John Wiley & Sons, Inc. Biopoly 54: 159–167, 2000

Keywords: *peptide conformation; dipropylglycine peptides; extended C_5 conformations; peptide crystal structure; nmr of peptides*

INTRODUCTION

The introduction of a second alkyl substituent at the C^α carbon atom in $C^{\alpha,\alpha}$ dialkylated glycines results in a dramatic restriction in the stereochemically allowed conformational space for these residues. The prototype residue, α-aminoisobutyric acid (Aib), α,α-dimethylglycine, has been shown by extensive crystallographic studies to favor left- or right-handed 3_{10}/α-helical conformations in a wide variety of peptides of differing lengths and sequences.[1,2] Indeed, Aib residues with very few exceptions almost invariably adopt local conformations that lie in the helical region of ϕ,ψ space ($\phi = \pm 60°$, $\psi = \pm 30°$). Extension of the alkyl chains results in the somewhat surprising observation that fully extended conformations ϕ ψ 180° are preferred in homooligopeptides of the Aib homologs (α,α-diethylglycine, Deg, and α,α-di-*n*-propylglycine, Dpg).[3–6] Indeed, early crystal structure determination of Dpg homooligomers yielded the first structural characterization of fully extended, C_5 conformations in peptides.[5] Theoretical calculations suggested that for the higher α,α dialkylglycines (Dpg and α,α-di-*n*-butylglycine, Dbg), the energy minima in fully extended regions of ϕ,ψ space are significantly deeper than the minima in the helical regions. Theoretical analysis also revealed a pronounced bond angle ($NC^\alpha C'$, τ) dependence at the tetrahedral C^α carbon atom, with helical conformations being favored for values of τ between 110° and 113° and fully extended conformations being preferred for values of τ between 101° and 105°.[5,7,8] Theoretical calculations suggest that the key difference between Aib and the higher α,α-dialkylglycine is the relative ordering of energy minima in the helical and the fully extended regions of the ϕ,ψ space. In the case of Aib, the minimum in the helical region is more pronounced, whereas the difference between the two conformations are smaller in the case of the higher dialkylglycines. In the case of Dpg, the majority of available examples correspond to heteromeric sequences in which Dpg adopts helical conformations.[9–13] Interestingly, even in the homotripeptide Tfa–(Dpg)$_3$–DBH (Tfa: trifluoroacetyl) the three Dpg residues adopt helical conformations.[14] The only examples of Dpg in a fully extended conformation are in the sequences of Tfa–Dpg–DBH,[3] Tfa–(Dpg)$_2$–DBH,[3] For–Met–Dpg–Phe–OMe,[15] Boc–Leu–Dpg–Val–OMe[16] (Mol. A), and Boc–Gly–Dpg–Gly–OH.[13] It is particularly interesting that in the sequence Boc–Leu–Dpg–Val–OMe, of the two molecules in the asymmetric unit, one molecule has the Dpg in a fully extended conformation ($\phi = 176°$, $\psi = -180°$) while the other one has Dpg in a local helical conformation ($\phi = 62.8°$, ψ

$= 39.6°$).[16] The coexistence of both conformations in the same crystal suggests that the energy differences between the two forms are likely to be very small. The possibility that the higher α,α- dialkylglycines (Dxg) may be used to stabilize both helical and fully extended conformations is of special importance in the area of *rational peptide design*. It is therefore necessary to define the conditions of sequence and chain length, which act as a determinant of the specific conformations of Dxg residues. We have therefore chosen to examine short synthetic peptides of defined sequence with a view toward stabilizing fully extended conformations in the Dxg peptides.

This paper describes conformational studies on valine-rich sequences containing a single guest Dpg residue. Oligovaline sequences have high tendency to adopt extended β-sheet conformations and have been widely investigated in the literature.[17–22] Nuclear magnetic resonance studies on the peptide sequences Boc–Val–Dpg–Val–OMe **(3)**, Boc–Val–Val–Dpg–Val–OMe **(4),** and Boc–Val–Val–Dpg–Val–Val–OMe **(5)** support the existence of C_5 conformations at Dpg in solution. Crystal structure analysis of the tripeptide Boc–Val–Dpg–Val–OMe also reveals a fully extended conformation at the Dpg residue.

EXPERIMENTAL

The peptides were assembled by conventional solution phase procedures using protocols described previously.[23] The Boc group was used for N-terminal protection and the C-terminus was protected as a methyl ester (OMe). Deprotections were performed using 98% formic acid while saponifications were carried out using 4N sodium hydroxide solution and methanol. Couplings were mediated by dicyclohexylcarbodiimide–1-hydroxybenzotriazole (DCC/HOBt). Dpg and H–Dpg–OMe · HCl were synthesized as described previously.[23] All intermediate peptides were characterized by ^{1}H-nmr (80 MHz, 400 MHz), thin layer chromatography (TLC), and used without further purification.

Synthesis of Peptides

Boc–Val–Dpg–OMe (1). Boc–Val–OH (4.3g, 20 mmol) was dissolved in dichloromethane (DCM; 20 mL). H–Dpg–OMe (5.20 g, 30 mmol) obtained from its ester hydrochloride was added, followed by DCC (4.0g, 20mmol). The reaction mixture was stirred at room temperature for 2 days. DCM was removed in vacuo. The residue was taken up in ethyl acetate (about 25 mL). The precipitated *N,N'*-dicyclohexylurea (DCU) was filtered. The organic layer was washed with excess of brine solution, 2N HCl (2 × 50 mL), 1M sodium carbonate solution (2 × 50 mL) and again with brine. The solution was then dried over anhydrous sodium

sulfate and evaporated in vacuo. The dipeptide **1** was obtained as a gum weighing 6.0 g (16 mmol, 80%).

80 MHz ^{1}H-NMR (CDCl$_3$, δ ppm). 0.8–0.93 (12H, m, Dpg C$^\delta$H$_3$/ Val C$^\gamma$H$_3$s), 1.2 (4H, m, Dpg C$^\gamma$H$_2$), 1.5 (9H, s, Boc CH$_3$), 1.6 (1H, m, Val C$^\beta$H), 2.4, 2.3 (4H, m, Dpg C$^\beta$H$_2$), 3.70 (3H, s, OCH$_3$), 4.1 (1H, m, Val C$^\alpha$H), 4.7 (1H, d, Val NH), 6.8 (1H, s, Dpg NH).

Boc–Val–Dpg–OH (2). Six grams (16 mmol) of peptide **1** was saponified using MeOH (20 mL) and 4N NaOH (18 mL). The reaction mixture was stirred at room temperature and its course followed by TLC. After 4 days, MeOH was evaporated and the residue taken in water. The aqueous solution was washed with ether (2 × 40 mL). The aqueous layer was neutralized with 2N HCl and extracted with ethyl acetate. The ethyl acetate extract was dried over anhydrous sodium sulfate and evaporated in vacuo to yield 5.0 g (14 mmol, 87.5%) of dipeptide acid **2**.

Boc–Val–Dpg–Val–OMe (3). Five grams (14 mmol) of peptide **2** was dissolved in dimethylformamide (DMF; 5 mL). H–Val–OMe isolated from 4.67 g (28 mmol) of its hydrochloride was added, followed by DCC (2.8g, 14 mmol) and HOBt (1.9g, 14 mmol). The reaction was stirred at room temperature for 3 days. DCU was filtered and the work up was similar to one described for **1**. The peptide **3** was obtained as a yellowish solid weighing 4.7 g (10 mmol, 71%).

The crude peptide was purified by medium pressure liquid chromatography (MPLC) on a reverse phase C$_{18}$ column (40–60 μ) using a gradient of MeOH/H$_2$O. Homogeneity of the peptide was subsequently demonstrated by analytical HPLC on a reverse phase (C$_{18}$, 5 μ) column; mp: 102–105°C. The peptide was characterized by complete assignment of the ^{1}H-nmr spectrum.

80 MHz ^{1}H-NMR (CDCl$_3$, δ ppm). 0.8–0.9 (18H, m, Dpg C$^\delta$H$_3$/ Val C$^\gamma$H$_3$s), 1.26 (4H, m, Dpg C$^\gamma$H$_2$), 1.5 (9H, s, Boc CH$_3$), 1.6 (2H, m, Val 1/ 3 C$^\beta$H), 2.4, 2.3 (4H, m, Dpg C$^\beta$H$_2$), 3.70 (3H, s, OCH$_3$), 4.0, 4.5 (2H, m, Val 1/ 3 C$^\alpha$H), 4.8 (1H, d, Val 1 NH), 6.52 (1H, d, Val 3 NH), 7.03 (1H, s, Dpg NH).

H–Val–Dpg–Val–OMe (3a). The amount of 4.7 g (10 mmol) of **3** was taken in 15 mL of 98% formic acid and the reaction mixture tightly stoppered. The reaction was monitored by TLC. After 8 h, formic acid was evaporated in vacuo and the residue was dissolved in water. The solution was washed with diethyl ether (2 × 30 mL). The aqueous layer was neutralized with sodium carbonate solution and extracted with ethyl acetate. The organic extract was dried over anhydrous sodium sulfate and evaporated in vacuo, to yield 2.4 g (6.5 mmol, 65%) of the tripeptide free base **3a** as a gum.

Boc–Val–Val–Dpg–Val–OMe (4). The amount of 1.4 g (6.5 mmol) of Boc–Val–OH was dissolved in DMF (4 mL). 2.4 g (6.5 mmol) of **3a** was added, followed by DCC (1.3g, 6.5 mmol) and HOBt (0.81g, 6.5 mmol). The reaction was

stirred at room temperature for 5 days. DCU was filtered and the work up was similar to one described for **1** to yield 2.8g (5 mmol, 76 %) of the tetrapeptide ester **4** as a white solid.

The crude peptide was purified by MPLC on a reverse phase C$_{18}$ column (40–60 μ) using a gradient of MeOH/H$_2$O. Homogeneity of the peptide was subsequently demonstrated by analytical HPLC on a reverse phase (C$_{18}$, 5 μ) column; mp: 101–103°C. The peptide was characterized by the complete assignment of the 400 MHz ^{1}H nmr spectrum.

400 MHz ^{1}H-NMR (CDCl$_3$, δ ppm). 0.8–0.98 (24H, m, Dpg C$^\delta$H$_3$ s/ Val 1/ 2/ 4 C$^\gamma$H$_3$s), 1.26 (4H, m, Dpg C$^\gamma$H$_2$), 1.49 (9H, s, Boc CH$_3$), 1.6 (2H, m, Val 4 C$^\beta$H), 2.15, 2.20 (8H, m, Val 1/ 2 C$^\beta$Hs), 2.15, 2.52 (4H, m, Dpg C$^\beta$H$_2$), 3.75 (3H, s, OCH$_3$), 3.9 (1H, m, Val 1 C$^\alpha$H), 4.3 (1H, m, Val 2 C$^\alpha$H), 4.52 (1H, m, Val 4 C$^\alpha$H), 5.05(1H, d, Val 1 NH), 6.3 (1H, d, Val 4 NH), 6.48 (1H, d, Val 2 NH), 7.05 (1H, s, Dpg 3 NH).

Boc–Val–Val–Dpg–Val–OH (4a). Peptide **4** (2.8g, 5 mmol) was saponified using 20 mL of MeOH and 4N NaOH (5 mL). The reaction was monitored by TLC. After 3 days the reaction was worked up as described for **2** to yield 2.2 g (4 mmol, 80%) of the tetrapeptide acid **4a** as a white solid.

Boc–Val–Val–Dpg–Val–Val–OMe (5). The amount of 2.2g (4 mmol) of **4a** was dissolved in DMF (6 mL). H–Val–OMe isolated from 2.6 g (8 mmol) of its hydrochloride was added, followed by DCC (0.8 g, 4 mmol) and HOBt (0.54 g, 4 mmol). The reaction was stirred at room temperature for 5 days. DCU was filtered and the workup was similar to that described for **1** to yield 2.0 g (3 mmol, 75 %) of the pentapeptide ester **5** as a white solid.

The crude peptide was purified by MPLC on a reverse phase C$_{18}$ column (40–60 μ) using a gradient of MeOH/H$_2$O. Homogeneity of the peptide was subsequently demonstrated by analytical HPLC on a reverse phase (C18, 5μ) column; mp: 115–117°C. The peptide was characterized by complete assignment of the 400 MHz ^{1}H-nmr spectrum.

400 MHz ^{1}H-NMR (CDCl$_3$, δ ppm). The amount of 0.8–1.0 (30H, m, Dpg C$^\delta$H$_3$ s/ Val 1/ 2/ 4 / 5 C$^\gamma$H$_3$s), 1.24 (4H, m, Dpg C$^\gamma$H$_2$), 1.50 (9H, s, Boc CH$_3$), 1.6, 2.20 (4H, m, Dpg C$^\beta$H$_2$), 2.15 (1H, m, Val 1 C$^\beta$H), 2.21–2.26 (2H, m, Val 4/ 5 C$^\beta$H), 2.23 (1H, m, Val 2 C$^\beta$H) 3.70 (3H, s, OCH$_3$), 3.88 (1H, m, Val 1 C$^\alpha$H), 4.2 (1H, m, Val 2 C$^\alpha$H), 4.35 (1H, m, Val 4 C$^\alpha$H), 4.5 (1H, m, Val 5 C$^\alpha$H), 5.05(1H, d, Val 1 NH), 6.52 (2H, d, Val 2/ 4 NH), 6.82 (1H, d, Val 5 NH), 7.08 (1H, s, Dpg 3 NH).

Spectroscopic Studies

All nmr studies were carried out on a Bruker AMX-400 spectrometer. Peptide concentrations were in the range of 7–8 m^M and the probe temperature was maintained at 298 K. Resonance assignments were done using two- dimensional (2D) rotating frame nuclear Overhauser effect (ROESY) spectra.[24] The 2D data was collected in phase sensitive mode using the time proportional phase incremen-

Table I   Torsion Angles (°) for Boc–Val–Dpg–Val–OMe[a]

Residue	ϕ	ψ	ω	χ^1	χ^2
Val[1]	−69.4	−24.4	177.8	153.1*	−62.3*
				66.8	−62.3
Dpg	−176.0	−180.0	−177.3	63.3, −179.0	−55.0, −166.1
Val[3]	−94.0	145.0	−176.2	171.1	−62.0

[a] The torsional angles for rotation about bonds of the peptide backbone (ϕ, ψ, ω) and about the bonds in the Dpg side chains (χ^1, χ^2) are defined following the IUPAC-IUB Commission on Biochemical Nomenclature, *Biochemistry* 1970, 9, 3471–3479. Estimated standard deviations ~1.0°.

[b] This value corresponds to the atom with occupancy 0.6 while the other value corresponds to the atom with occupancy 0.4.

tation method. Five hundred twelve data points with 64 transients were collected. Spectral widths were in the range of 4500 Hz with a spin–lock time of 300 ms. Zero filling was done to yield data sets of 1K × 1K using a square sine-bell window.

X-Ray Studies

Crystals of peptide **3** were grown from an ethyl acetate/hexane/ethanol (2:1:3) mixture by slow evaporation at room temperature. Peptide **3** ($C_{24}H_{45}N_3O_6$) crystallized in the orthorhombic space group $P2_12_12$, a (Å) = 12.324(2), b (Å) = 20.835(4), c (Å) = 11.253(2), V (Å^3) = 2889.4 (9) with Z = 4, M_w = 471.6, ρ= 1.08, $F(ooo)$ = 1032, observed reflections [$I > 2\sigma$ (I)] = 1950, R [$I > 2\sigma$ (I)] = 0.063, R_W = 0.28. The x-ray intensity measurements were made at room temperature on an Enraf-Nonius CAD4 diffractometer equipped with a graphite monochromator, using CuKα radiation in $\omega/2\theta$ scan mode. Accurate unit cell parameters were obtained by a least squares fit of the θ values for several high angle reflections in the range θ = 15°–22°. Intensity data were collected up to $2\theta_{max}$ = 140°. Three standard reflections were monitored for every 100 reflections and ensured no significant variation of intensities during data collection. Intensity data were corrected for Lorentz, polarization, and absorption effects.

The structure was solved using the direct methods package SHELXS-86[25] and refined isotropically and anisotropically using the program package SHELXL-93.[26] During refinement the side chain atom $C_1^{\gamma 1}$ of valine(1) showed positional disorder, suggestive of its presence in two alternative positions with equal occupancy. Refinement of the positional and isotropic thermal parameters for these alternative sites of $C_1^{\gamma 1}$ with occupancies fixed at 0.5 yielded reasonable thermal parameters. At this stage, the thermal parameters were kept fixed and occupancies were refined. The refinement indicated that their relative occupancy factors were more close to the ratio 0.6:0.4. Further refinement was therefore carried out with fixed occupancy factors 0.6 and 0.4 respectively for two alternative sites of $C_1^{\gamma 1}$. Full matrix anisotropic least-squares refinement was done on all the nonhydrogen atoms (except the disordered atoms). All the hydrogens except for the disordered atoms were geometrically fixed and included as riding atoms with fixed

isotropic displacement parameters in the structure factor calculations. The function minimized was Σw $(|F_o|^2 - |F_c|^2)^2$. The final R factor is 0.063. Tables of atomic coordinates, bond lengths, bond angles, anisotropic temperature factors, and H-atom coordinates for peptide **3** are available from the authors on request. Coordinates are also being deposited in the Cambridge Crystallographic Data File. The torsional angles and hydrogen bonds are listed in Tables I and II, respectively.

RESULTS AND DISCUSSION

NMR Analysis of Peptide Conformations

The three peptides Boc–Val–Dpg–Val–OMe (**3**), Boc–Val–Val–Dpg–Val–OMe (**4**), and Boc–Val–Val–Dpg–Val–Val–OMe (**5**) were investigated in CDCl$_3$ and DMSO solutions. Resonance assignments in CDCl$_3$ were accomplished in a routine manner using ROESY spectra[24] and the known upfield position of the urethane NH in this solvent. The resonance assignments in DMSO were obtained from solvent titration experiments.[27, 28] Figure 1 shows the effect of addition of increasing concentrations of the strongly hydrogen-bonding cosolvent DMSO to the CDCl$_3$ solutions. In all the three cases, it is observed

Table II   Hydrogen Bonds in the Crystal of Boc–Val–Dpg–Val–OMe

Type	N $\cdots$ O (Å)	H $\cdots$ O (Å)	N—H $\cdots$ O (°)
Intramolecular			
N2 $\cdots$ O$_2$	2.552	2.068	113
Intermolecular			
N3 $\cdots$ O$_1$[a]	2.877	2.020	159
N1 $\cdots$ O4[b]	3.265	2.388	165

[a] Equivalent positions: $x − 1/2$, $−y + 3/2$, $−z + 1$.
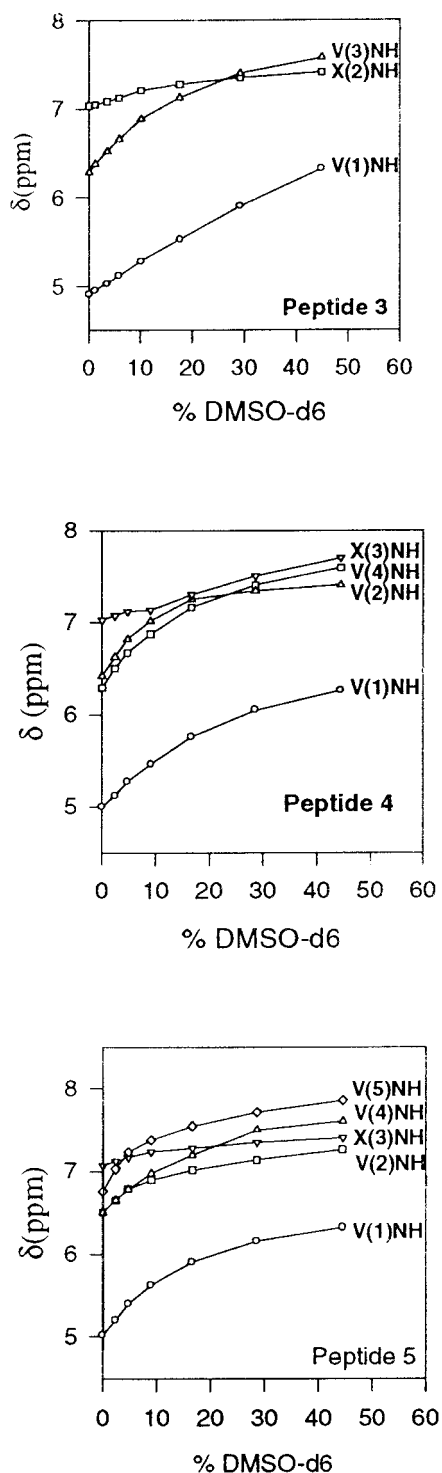[b] $x + 1/2$, $−y + 3/2$, $−z$.

FIGURE 1 Plots of NH chemical shifts of peptides **3** (top), **4** (middle), and **5** (lower), showing their dependence on DMSO concentration. (X = Dpg.).

that all the Val NH resonances show appreciable downfield shifts (δDMSO–δCDCl$_3$, $\Delta\delta$ = 0.9–2.0 ppm). In contrast, the Dpg NH resonances in peptides

3, **4**, and **5** are much less affected by the addition of DMSO (δDMSO–δCDCl$_3$, $\Delta\delta$ = 0.40–0.43 ppm), suggesting that these NH groups are significantly less accessible to the solvent. The solvent shielded nature of Dpg NH groups cannot be explained by invoking β-turn conformations in which Dpg occupies a corner (i + 1/i + 2) position since the NH group of these positions is exposed. In principle, in peptides **4** and **5**, β-turns involving the Val(1)–Val(2) segment can be invoked with the Dpg at the i + 3 position, with the NH group involved in a 4 → 1 hydrogen bond. This is unlikely since the Val–Val segment has a very low β-turn propensity. Furthermore, this possibility is excluded in peptide **3**, where Dpg is placed at position 2. A possible explanation for the reduced tendency of the Dpg NH to interact with DMSO in these three peptides is the occurrence of C$_5$ conformations at this residue. In a fully extended ($\phi \sim \psi \sim 180°$) C$_5$ conformation, the NH and CO groups of the Dpg residue are proximal, with the bond vectors almost perfectly parallel (Figure 2). In such a conformation, close approach of the sulfoxide moiety of DMSO is likely to be inhibited due to stereoelectronic effects. An alternative explanation that the Dpg NH is shielded due to the formation of a C$_7$ (γ-turn) conformation at the preceding valine residue in peptide **3** or β-turn conformation formed by the Val–Val segments preceding Dpg in peptides **4** and **5** was discarded, since there is no specific reason to have an appreciable population of folded C$_7$ conformations at these valine residues. Confirmation for the occurrence of valine residues in largely extended structures was obtained from ROESY spectra, which showed weak or unobservable interresidue N$_i$H $\leftrightarrow$ N$_{i+1}$H (d_{NN} connectivities) and strong interresidue C$_i$H $\leftrightarrow$ N$_{i+1}$H [$d_{\alpha N}$ nuclear Overhauser effects (NOEs)] for valine residues in peptides **4** and **5**. Figure 3 illustrates the partial
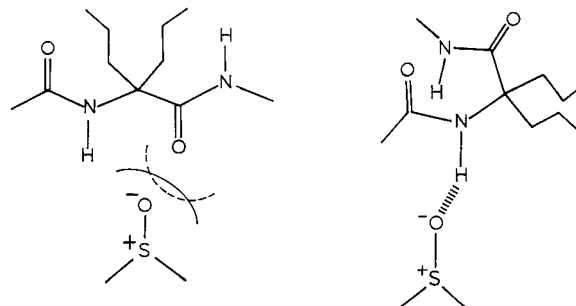

FIGURE 2 Schematic view of modes of solvation of exposed NH groups by DMSO in the C$_5$ (left) and helical (right) conformation. Note that in the C$_5$ conformation stereoelectronic factors will disfavor approach of the sulfoxide group.
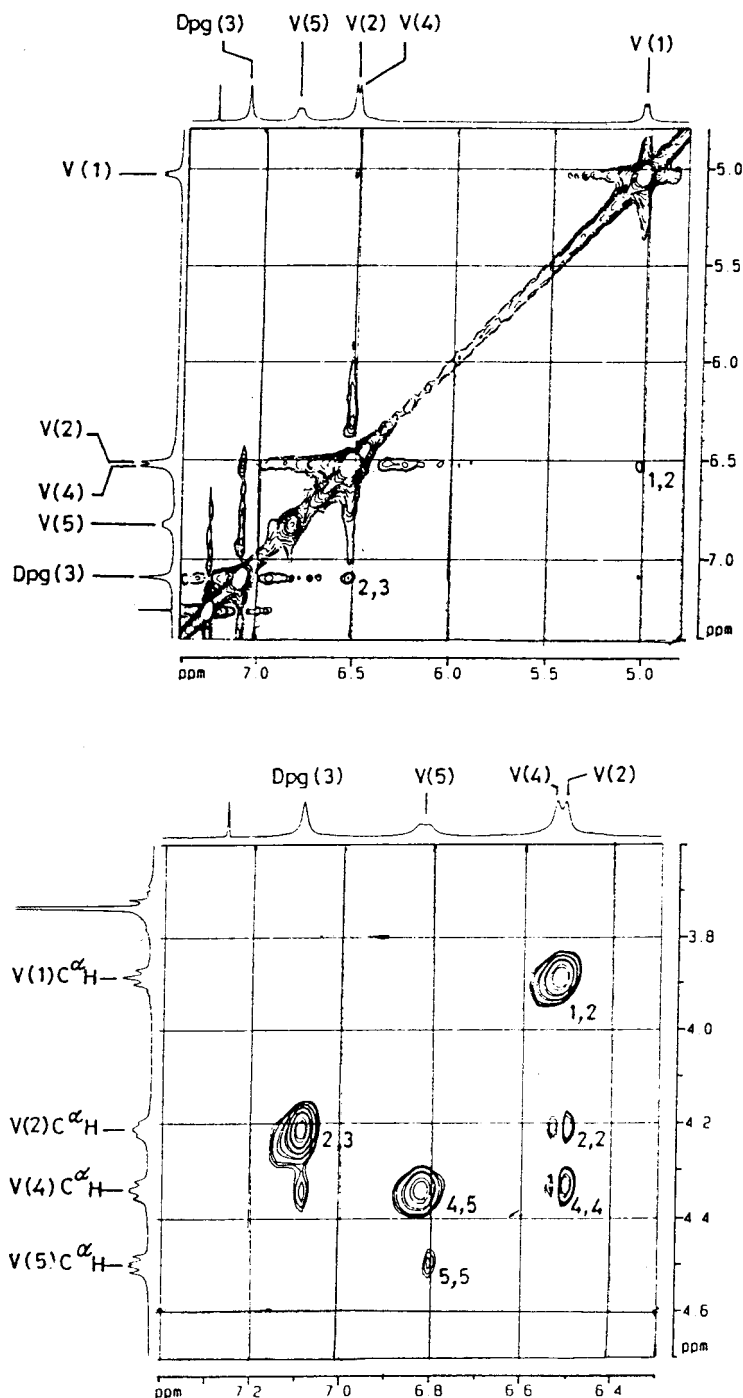
FIGURE 3 Partial 400 MHz ^{1}H–^{1}H ROESY spectra of peptide **5** in CDCl$_3$, showing N$_i$H $\leftrightarrow$ N$_{i+1}$H connectivities (top panel) and C$_i^\alpha$H $\leftrightarrow$ N$_{i+1}$H connectivities (lower panel). (X= Dpg.)

ROESY spectrum for the pentapeptide **5,** clearly demonstrating that $d_{\alpha N}$ NOEs are extremely intense, while d_{NN} NOEs are very weak. An important conclusion to emerge from the above results is that solvent perturbation of chemical shifts must be used with caution in delineating intramolecularly hydrogen bonded NH groups in peptides. In structures like helices and β-turns, nonhydrogen-bonded NH groups are also always accessible to solvation. In contrast, in fully extended conformations the local environment of NH groups acts as a deterrent to the approach of hydrogen-bond accepting solvents like DMSO.
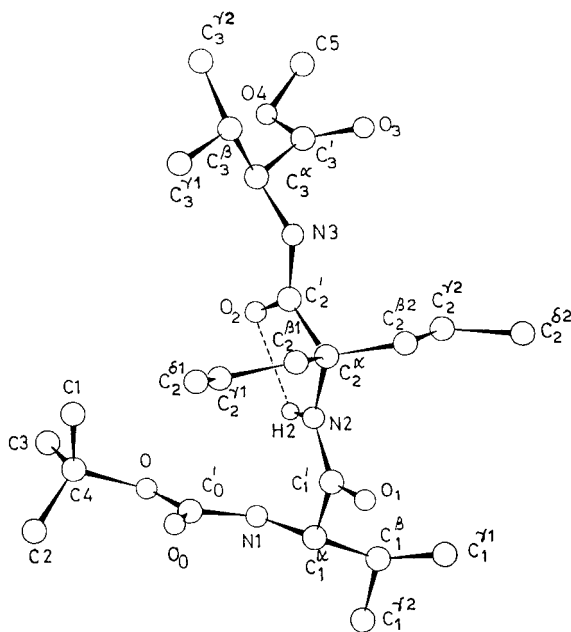
FIGURE 4 Molecular conformation of Boc–Val–Dpg–Val–OMe, **3**, in crystals. The dotted line indicates the C_5 N–H $\cdots$ O interaction.

In DMSO, the temperature coefficients of NH groups in peptides **3**–**5** reveals that all the valine resonances have $d\delta/dt$ values in the range of 3.3–5.3 ppb/K, characteristic of solvent-exposed NH groups. In contrast, the Dpg residues in all the three peptides exhibits low $d\delta/dt$ values characteristic of solvent-inaccessible NH groups [$-d\delta/dt$ (ppb/K) = 1.02 (**3**), 1.3 (**4**), and 1.3 (**5**)]. The low temperature coefficients for the Dpg NH groups may once again be interpreted as indicative of the absence of close approach by DMSO molecules.

Crystal Structure of Peptide

While attempts were made to crystallize all the three peptides, only peptide **3** readily yielded crystals suitable for x-ray diffraction. Two intermolecular hydrogen bonds, Val(3) N—H $\cdots$ O=C Val(1) and Val(1) N—H $\cdots$ O4 ester group, between symmetry-related molecules stabilize the crystal. Of these, the former interaction appears significantly stronger than the latter, as evidenced by the appeared shorter N $\cdots$ O distance (Table II). The molecular conformation of **3** in crystals and the packing arrangement are shown in Figures 4 and 5, respectively. The backbone torsion angles are listed in Table I. From the torsion angles at the Dpg residue, it is clear that the conformation is fully extended, while Val(1) adopts a local helical conformation and Val(3) is semiextended. The bond

angle τ Dpg(2) is 103.4°. Extended conformations at Dpg usually accommodate τ values of 101°–105°, while helical conformation are characterized by τ values of 110°–113°.[8] It should be noted in a related peptide Boc–Leu–Dpg–Val–OMe, two molecules were present in the asymmetric unit, one of which adopted a local helical conformation while the other was fully extended at the Dpg residue.[16] Hydrogen-bond parameters for the C_5 interaction at Dpg are listed in Table II.

Correlation Between Solid State and Solution Conformations

Table III summarizes backbone torsion angles for Dpg residues in diverse peptides determined by x-ray diffraction in crystals. Nuclear magnetic resonance parameters in DMSO, NH chemical shifts, and temperature coefficients ($d\delta/dt$) are also listed. The Dpg residues fall into two distinct conformational classes, one being the fully extended C_5 conformation ($\phi \sim \psi \sim 180°$), while the other is characterized by helical ϕ, ψ values ($\phi = \pm 50°$, $\psi = \pm 50°$). All the four decapeptides in the series Boc–Gly–Dpg–Xxx–Val–Ala–Leu–Aib–Val–Ala–Leu–OMe (Xxx = Gly, Ala, Pro, and Leu) adopt largely helical conformation in crystals with Dpg(2) having ϕ, ψ values consistent with a right-handed helical structure.[10,11] In these cases Dpg residues are at the N-terminus of a peptide helix, thus leaving the Dpg NH accessible to the solvent. The NH chemical shift in all the helical Dpg
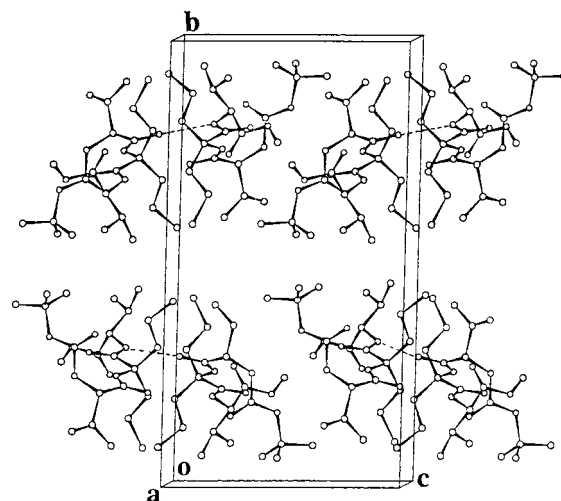

FIGURE 5 Packing of peptide **3** viewed down the <u>a</u> axis. Broken lines indicate the intermolecular hydrogen bond between Val(3) N–H and Val(1) C=O groups. The second intermolecular hydrogen bond (Table II) is not shown since it lies in a direction perpendicular to the projected view.

Table III   Comparison of Conformational Angles in the Crystal State with NMR Parameters of Dpg Residues

Peptides	Conformational Angles (°)		NMR Parameters	
	ϕ	ψ (Ref.)	δ (ppm)[a]	$-d\delta/dt$ (ppb/°K)[b] (Ref.)
Tfa–(**Dpg**)$_2$–OtBu/DBH	179.5[c]	169.4[c] (3)	8.01, 6.88	1.6, 1.2[c] (5)
	172.5	−179.4		
			8.04, 7.40	1.5, 1.0 (5)
Tfa–(**Dpg**)$_3$–OtBu	—	—	6.85	1.1
				1.5, 0.8, (5),
			8.05, 7.42	0.9,
Tfa–(**Dpg**)$_4$–OtBu	—	—	7.34, 6.84	0.9
Tfa–(**Dpg**)$_3$–DBH	±54.8	±39.4	—	—(14)
	±59.9	±10.2	—	—
	±48.3	±32.9	—	—
Boc–Leu–**Dpg**–Val–OMe Mol. A	176.0	−180.0	—	—(16)
Mol. B	62.8	39.6	—	—
For–Met–**Dpg**–Phe–OMe	173.1	179.0 (13)	7.38	1.0 (15)
Boc–Ala–**Dpg**–Ala–OMe	66.2	19.3 (27)	7.50	1.8 (29)
Boc–Gly–**Dpg**–Ala–Val–Ala–Leu–Aib–Val–Ala–Leu–OMe	−46.0	−35.0 (8)	7.94	4.2[f]
Boc–Gly–**Dpg**–Leu–Val–Ala–Leu–Aib–Val–Ala–Leu–OMe	−51.0	−47.0 (8)	8.05	4.3[f]
Boc–Gly–**Dpg**–Pro–Val–Ala–Leu–Aib–Val–Ala–Leu–OMe	−52.0	−51.0 (8)	8.69	6.3[f]
Boc–Gly–**Dpg**–Gly–Val–Ala–Leu–Aib–Val–Ala–Leu–OMe	−53.0	−50.0 (9)	7.87	4.0[f]
Boc–Gly–**Dpg**–Gly–OH	178.0	171.0 (11)	7.50	1.5[d]
Boc–Gly–**Dpg**–Gly–Gly–**Dpg**–Gly–NHMe	−54.0	−46.0 (10)		
	56.0	32.0	7.73, 7.73	4.9, 3.8 (12)
Boc–Val–**Dpg**–Val–OMe[e]	−176.0	−180.0	7.43	1.02
Boc–Val–Val–**Dpg**–Val–OMe[e]	—	—	7.45	1.30
Boc–Val–Val–**Dpg**–Val–Val–OMe[e]	—	—	7.50	1.40

[a] NH chemical shift values in DMSO.
[b] $d\delta/dt$ measured in DMSO.
[c] Crystallographic studies on Tfa–(Dpg)$_2$–DBH.
[d] Values for Boc–Gly–Dpg–Gly–OBzl (unpublished).
[e] This study.
[f] Submitted for publication.

residues is rather low (>7.8 δ) and $d\delta/dt$ values are all rather large ≥ 4.0 ppb/K. In the peptide Boc–Gly–Dpg–Gly–Gly–Dpg–Gly–NHMe, both Dpg residues adopt helical conformations of opposite chirality in crystals[12]; while Dpg(2)NH does not participate in any intramolecular hydrogen bond; the potential hydrogen bond involving Dpg(5)NH is disrupted by solvent invasion. Interestingly, both NH groups in DMSO have a δ value of 7.7 ppm and have relatively high $d\delta/dt$ values (3.8 and 4.9 ppb/K). The data in Table III clearly indicates that in the case of extended conformations the Dpg NH resonances appear at significantly higher field in DMSO δ ≤ 7.5 and have very low temperature coefficients ($d\delta/dt$ ≤ 1.8 ppb/

K). The substituent shifts of Dpg NH groups, when the residue is protected with a Tfa group, are abnormally low (∼ 8.0δ), suggesting an overriding substituent effect. Inspection of the chemical shifts of peptides **3**, **4**, and **5**, and $d\delta/dt$ values measured in DMSO suggest that the sequences examined in the present studies indeed stabilize Dpg conformations that are fully extended. The observation of a fully extended conformation at Dpg in the crystal structure of **3** provides support for the observed correlation between conformational parameters determined in crystals and nmr parameters determined in solution.

The growing body of evidence on the conformation of Dpg-containing peptides provides some clues

as to the factors that stabilize either helical or fully extended conformations. In sequences where the flanking residues have a strong tendency to adopt extended structures, C_5 conformations at Dpg may in fact be predominant. This feature is apparent in the present studies in which Dpg has been inserted into valine-rich sequences. In helix-promoting situations, Dpg can be comfortably accommodated into a helical conformation. In the case of the tripeptide Boc–Ala–Dpg–Ala–OMe, the results summarized in Table III suggests that while the crystal structure reveals a helical Dpg residue, in DMSO solution an extended conformation is favored. Interestingly, in the tripeptide For–Met–Dpg–Phe–OMe, an extended structure is characterized in crystals while in the tripeptide Boc–Leu–Dpg–Val–OMe the single crystal accommodated both helical and extended Dpg conformations. In the present study, the closely related peptide Boc–Val–Dpg–Val–OMe has been shown to have an extended Dpg conformation. Clearly, the extended and helical conformations of Dpg correspond to minima of comparable energy. Recent molecular dynamics simulations using "flat bottom" harmonic potentials have emphasized the relationship between C^α bond angles and backbone conformations, and pointed to limitations in the use of rigid geometry approaches in energy calculations.[8] Precise conformational preferences at Dpg residues are determined by subtle sequence and environmental factors. The present study suggests that in contexts that strongly promote extended conformations, it may indeed be possible to stabilize C_5 structures at Dpg even in heteromeric sequences.

REFERENCES

1. Prasad, B. V. V.; Balaram, P. CRC Crit Rev Biochem 1984, 16, 307–347.
2. Karle, I. L.; Balaram, P. Biochemistry 1990, 29, 6747–6756.
3. Bonora, G. M.; Toniolo, C.; Di Blasio, B.; Pavone, V.; Pedone, C.; Benedetti, E.; Lingham, I.; Hardy, P. M. J Am Chem Soc 1984, 106, 8152 – 8156.
4. Benedetti, E.; Barone, V.; Bavoso, A.; Di Blasio, B.; Lelj, F.; Pavone, V.; Pedone, C.; Bonora, G. M.; Toniolo, C.; Leplawy, M. T.; Kaczmarek, K.; Redlinski, A. Biopolymers 1988, 27, 357–371.
5. Benedetti, E.; Toniolo, C.; Hardy, P. M.; Barone, V.; Bavoso, A.; Di Blasio, B.; Grimaldi, P.; Lelj, F.; Pavone, V.; Pedone, C.; Bonora G. M.; Lingham, I. J Am Chem Soc 1984, 106, 8146 – 8152.
6. Toniolo, C.; Benedetti. E. Macromolecules 1991, 24, 4004 – 4009.
7. Barone, V.; Lelj, F.; Bavoso, A.; Di Blasio, B.; Grimaldi, P.; Pavone, V.; Pedone, C. Biopolymers 1985, 24, 1759 –1767.
8. Cirilli, M.; Coiro, V. M.; Di Nola, A.; Mazza, F. Biopolymers 1998, 46, 239 –244.
9. Karle, I. L.; Rao, R. B.; Prasad, S.; Kaul, R.; Balaram, P. J Am Chem Soc 1994, 116, 10355–10361.
10. Karle, I. L.; Gurunath, R.; Prasad, S.; Kaul, R.; Rao, R. B.; Balaram, P. J Am Chem Soc 1995, 117, 9632–9637.
11. Karle, I. L.; Rao, R. B.; Kaul, R.; Prasad, S.; Balaram, P. Biopolymers 1996, 39, 75– 84.
12. Karle, I. L.; Kaul, R.; Rao, R. B.; Ragothama, S.; Balaram, P. J Am Chem Soc 1997, 119, 12048 –12054.
13. Datta, S.; Kaul, R.; Rao, R. B.; Shamala, N.; Balaram, P. J Chem Soc Perkin Trans 2 1997, 1659 –1664.
14. Di Blasio, B.; Pavone, V.; Isernia, C.; Pedone, C.; Benedetti, E.; Toniolo, C.; Hardy, P. M.; Lingham, I. J Chem Soc Perkin Trans 2 1992, 523–526.
15. Dentino, A. R.; Raj, P. A.; Bhandary, K. K.; Wilson, M. E.; Levine, M. J. J Biol Chem 1991, 266, 18460–18468.
16. Prasad, S.; Mitra, S.; Subramanian, E.; Velmurugan, D.; Rao R. B.; Balaram, P. Biochem Biophys Res Commun 1994, 198, 424 –430.
17. Balcerski, J. S.; Pysh, E. S.; Bonora, G. M.; Toniolo, C. J Am Chem Soc 1976, 98, 347–3473.
18. Baron, M. H.; de Loze, C.; Toniolo, C.; Fasman, G. D. Biopolymers 1979, 18, 411– 424.
19. Toniolo, C. Macromolecules 1978, 11, 437– 438.
20. Toniolo, C.; Bonora, G. M.; Mutter, M. J Am Chem Soc 1979, 101, 450– 454.
21. Toniolo, C.; Bonora, G. M.; Salardi, C. Int J Biol Macromol 1981, 3, 377–383.
22. Moretto, V.; Crisma, M.; Bonora, G. M.; Toniolo, C.; Balaram, H.; Balaram, P. Macromolecules 1989, 22, 2939 –2944.
23. Prasad, S.; Rao, R. B.; Balaram, P. Biopolymers 1995, 35, 11–20.
24. Wüthrich, K. NMR of Protein and Nucleic Acids; John Wiley & Sons: New York, 1986.
25. Sheldrick, G. M. SHELXS 86. A Program for Crystal Structure Solution; Institute of Anorganische, Chemie der Universitat: Gottingen, Germany, 1986.
26. Sheldrick, G. M. SHELXL 93. A Program for Crystal Structure Determination; University of Cambridge: Cambridge, England, 1993.
27. Pitner, T. P; Urry, D. W. J Am Chem Soc 1972, 94, 1399 –1400.
28. Iqbal, M.; Balaram, P. J Am Chem Soc 1981, 103, 5548 –5552.
29. Crisma, M. Coiro, V. M.; Di Nola, A.; Mazza, F. Biopolymers 1998, 46, 239 – 244.